

UCSF

UC San Francisco Previously Published Works

Title

Neoadjuvant sipuleucel-T induces both Th1 activation and immune regulation in localized prostate cancer.

Permalink

<https://escholarship.org/uc/item/3cp511qx>

Journal

Oncoimmunology, 8(1)

ISSN

2162-4011

Authors

Hagihara, Katsunobu
Chan, Stephen
Zhang, Li
[et al.](#)

Publication Date



2019

DOI

10.1080/2162402x.2018.1486953

Peer reviewed

Neoadjuvant sipuleucel-T induces both Th1 activation and immune regulation in localized prostate cancer

Katsunobu Hagihara ^{a,b}, Stephen Chan^a, Li Zhang^{a,c}, David Y. Oh^{a,b}, Xiao X. Wei^{a,d}, Jeffrey Simko^{a,b}, and Lawrence Fong ^{a,b}

^aDivision of Hematology and Oncology, University of California, San Francisco, CA, USA; ^bHelen Diller Family Comprehensive Cancer Center, University of California, San Francisco, San Francisco, CA, USA; ^cDepartment of Epidemiology and Biostatistics, University of California, San Francisco Helen Diller Family Comprehensive Cancer Center, San Francisco, CA, USA; ^dLank Center for Genitourinary Oncology, Dana-Farber Cancer Institute, Harvard Medical School, Boston, MA, USA

ABSTRACT

Sipuleucel-T is the only FDA-approved immunotherapy for metastatic castration-resistant prostate cancer. The mechanism by which this treatment improves survival is not fully understood. We have previously shown that this treatment can induce the recruitment of CD4 and CD8 T cells to the tumor microenvironment. In this study, we examined the functional state of these T cells through gene expression profiling. We found that the magnitude of T cell signatures correlated with the frequency of T cells as measured by immunohistochemistry. Sipuleucel-T treatment was associated with increased expression of Th1-associated genes, but not Th2-, Th17- or Treg-associated genes. Post-treatment tumor tissues with high CD8+T cell infiltration was associated with high levels of CXCL10 expression. On in situ hybridization, CXCL10+ cells colocalized with CD8+T cells in post-treatment prostatectomy tumor tissue. Neoadjuvant sipuleucel-T was also associated with upregulation of immune inhibitory checkpoints, including CTLA4 and TIGIT, and downregulation of the immune activation marker, dipeptidyl-peptidase, DPP4. Treatment-associated declines in serum PSA were correlated with induction of Th1 response. In contrast, rises in serum PSA while on treatment were associated with the induction of multiple immune checkpoints, including CTLA4, CEACAM6 and TIGIT. This could represent adaptive immune resistance mechanisms induced by treatment. Taken together, neoadjuvant sipuleucel-T can induce both a Th1 response and negative immune regulation in the prostate cancer microenvironment.

ARTICLE HISTORY

Received 7 May 2018
Revised 1 June 2018
Accepted 6 June 2018

KEYWORDS

Th1; CD8; prostate cancer; checkpoint inhibition; resistance; immunomonitoring; therapeutic vaccination

Introduction

Sipuleucel-T (Provenge) is an autologous cellular vaccine approved for the treatment of metastatic castration resistant prostate cancer in patients who have asymptomatic or minimally symptomatic disease. Sipuleucel-T is designed to stimulate an anti-tumor immune response against prostatic acid phosphatase (PAP), a tumor-associated antigen expressed in over 95% of prostate adenocarcinoma. It was recently appreciated that sipuleucel-T also induces humoral immune responses against non-target (non-PAP) tumor antigens via antigen spread¹ and this broadening of the immune response may contribute to the clinical efficacy of sipuleucel-T in the extension of overall survival.^{2,3}

To investigate the effect of sipuleucel-T in the tumor microenvironment, we had conducted a phase II study of neoadjuvant sipuleucel-T in patients prior to radical prostatectomy. Immunohistochemical analysis showed that neoadjuvant sipuleucel-T induced T cell infiltration into the tumor (CD8⁺ > CD4⁺FOXP3⁻ > CD4⁺FOXP3⁺) with an activated phenotype (CD3⁺Ki67⁺, CD3⁺PD-1⁺) at the tumor interface⁴ More recently, utilizing deep sequencing of the TCRβ CD3 region in

the same patient cohort, we showed that neoadjuvant sipuleucel-T decreased the diversity of circulating TCR repertoire while increased the diversity of TCR repertoire in the tumor tissue. This resulted in a greater overlap between the peripheral and intratumoral TCR sequences, which may represent recruitment of antigen-specific T cells from the periphery into the tumor tissue.⁵

In the present study, we investigate functional capacity intratumoral immune cell populations in paired pre-treatment biopsy and post-treatment radical prostatectomy tissues. We show that sipuleucel-T upregulates multiple immune response categories, including promotion of a Th1 biased immune response as well as upregulation of immune checkpoint suppressors which are associated with divergent treatment-associated PSA changes.

Results

Neoadjuvant sipuleucel-T treatment induces a T cell expression profile in the tumor microenvironment

We examined the expression profile of formalin fixed paraffin embedded (FFPE) prostate tissues obtained pre- or

post-sipuleucel-T treated using the nCounter PanCancer Immune panel (Nanostring). Most genes in the panel appeared to be upregulated after treatment with sipuleucel-T, consistent with stimulation of an intratumoral immune response with treatment (Figure 1A). Upon closer examination, all immune response categories appeared to be upregulated after treatment with sipuleucel-T, with genes involved in leukocyte functions exhibiting the highest level of increase in expression (Figure 1B). Immune cell scores of lymphocytes infiltrated into the tumor microenvironment were calculated by nSolver software based on gene expression levels normalized to housekeeping genes⁶. The scores of total T cells, cytotoxic CD8 T cells, and helper T cells were significantly increased after sipuleucel-T treatment ($p = 0.02$, 0.05 and <0.01 , respectively), and there was a trend for increased total B cells post-treatment ($p = 0.11$, Figure 1C). When examining specific CD4 T cell subsets, the immune cell score of the Th1 subtype was significantly increased after treatment ($p = 0.03$), while the immune cell scores of Th2, Th17 and Treg subtypes were unchanged (Figure 1D). For all five paired cases examined, an upregulation of Th1/Th2 ratio was observed with treatment ($p < 0.01$, Figure 1E). We had previously shown that sipuleucel-T treatment was associated with an increase in infiltration of CD3+, CD4+Foxp3- and CD8+T cells into the tumor microenvironment⁴. To confirm reliability of the calculated lymphocyte scores, we assessed their correlation with CD3, CD8, Foxp3 and CD20 staining by immunohistochemistry (IHC), scored by the frequency of positive staining at the tumor interface. The total T cells, CD8 T cells and Treg scores were significantly correlated with IHC scores for CD3, CD8 and Foxp3, respectively ($p = 0.02$). There was a trend in correlation between the B cell score and CD20 staining on IHC ($p = 0.08$) (Supplemental Figure 1).

Chemokine changes associated with high intratumoral CD8+T cell infiltration following sipuleucel-T treatment

We hypothesized that chemokines produced in the tumor microenvironment served to attract CD8+T cells into the tumor and sought to identify chemokine genes differentially upregulated in high CD8+T cell infiltrated versus low CD8+T cell infiltrated post-treatment prostatectomy tumor tissues ($N = 14$). We found that CXCL10 was the most significantly differentially upregulated gene, followed by CXCL9 and CXCL11 (Figure 2A), suggesting that these cytokines – particularly CXCL10 – may promote the migration of CD8 T cells into the tumor microenvironment. To further investigate this possibility, we performed in situ hybridization in post-sipuleucel-T tumor tissues. CD8a expressing cells were localized close to CXCL10 expressing cells in the tumor microenvironment (Figure 2B), supporting its role in the attraction of CD8 +T cells. M1 macrophages have been reported to produce CXCL10.⁷ In keeping with this, the expression levels of genes associated with M1 macrophages (CD68, CD80 and CD86) were significantly correlated with CXCL10 gene expression (Supplemental Figure 2).

Serum PSA decline is associated with induction of Th1 response after sipuleucel-T treatment

We examined the association between treatment-related PSA change and immune cell scores determined by gene expression (Supplemental Table 1), where the data of PSA change were available in thirteen cases. Six (43%) patients had PSA decline with sipuleucel-T treatment (range of PSA decline: 5.3%–33.6%). Maximal PSA change was inversely correlated with Th1/total T cell ratio (Figure 3A), suggesting that infiltration of Th1 cells into the tumor microenvironment promotes PSA response. We also examined the modulation of

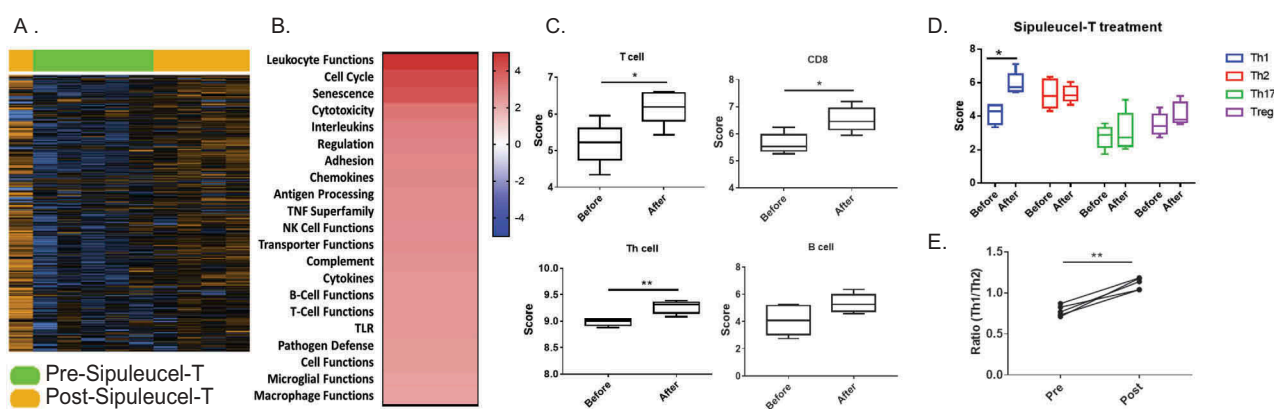


Figure 1. Gene expression of paired prostate tissues obtained pre- and post-sipuleucel-T treatment. (A) Post-sipuleucel-T vs. pre-sipuleucel-T gene expression analysis. Heatmap of the unsupervised clustering of normalized genes expressed, scaled to give all genes equal variance. Orange indicates high expression; blue indicates low expression. (B) Directed global significance immune cell scores (post-sipuleucel-T vs. pre-sipuleucel-T). The score values were calculated as the square root of the mean signed squared t-statistic for the genes in a gene set, with t-statistics derived from the linear regression underlying the differential expression analysis. (C) Immune gene scores of T cells, CD8+T cells, Th cells and B cells in prostate tumor tissues before and after sipuleucel-T treatment. Two-tailed paired t test was used to test for differences in mean Nanostring scores. (D) Scores of T cell subsets in prostate tumor tissues before and after sipuleucel-T treatment. Each T cell subset score was calculated based on the following genes; Th1 cells: CTLA4, LTA, IFNG, CD38, and CCL4; Th2 cells: PMCH; Th17 cells: IL26 and IL17A; Treg cells: FOXP3 and LILRA4. Two-tailed paired t test was used to test for differences in mean Nanostring scores. (E) Comparison of Th1/Th2 score ratios between pre- and post-sipuleucel-T treatment. Two-tailed paired t test was used to test for differences in mean Nanostring score ratios. (F) Correlation of immune cell scores by gene expression (X-axis) with IHC scores (Y-axis). For the IHC scores, CD3+, CD8+, Foxp3+ and CD20+ cells were quantified by digital image analysis at the tumor interface.

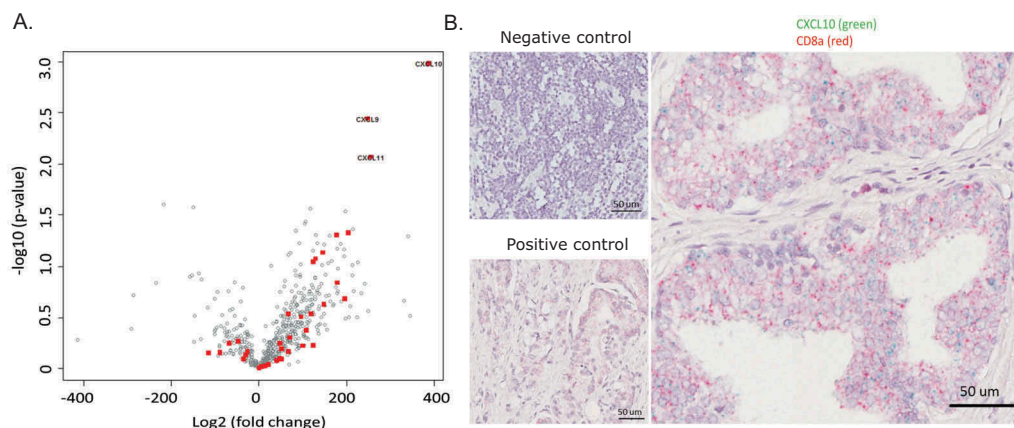


Figure 2. Intratumoral chemokine expression after sipuleucel-T treatment (n = 14). (A) Differential expression of immune-related genes in high vs. low CD8 T cell infiltrated cases are shown. Chemokine-related genes are shown in red. The X-axis represents log fold-difference which estimates a gene's differential expression (2^{Δ} (log fold change)-fold). (B) Localization of CXCL10 mRNA (green) and CD8a mRNA (red) expressing cells in the tumor microenvironment. The following probes were used in in situ hybridization. Negative control: DapB (bacterial dihydrodipicolinate reductase); positive control (green): POLR2A (encoding DNA-directed RNA polymerase II subunit RPB1); positive control (red): PPIB (human peptidylprolyl isomerase B). The section stained for CXCL10/CD8a is representative of fourteen cases.

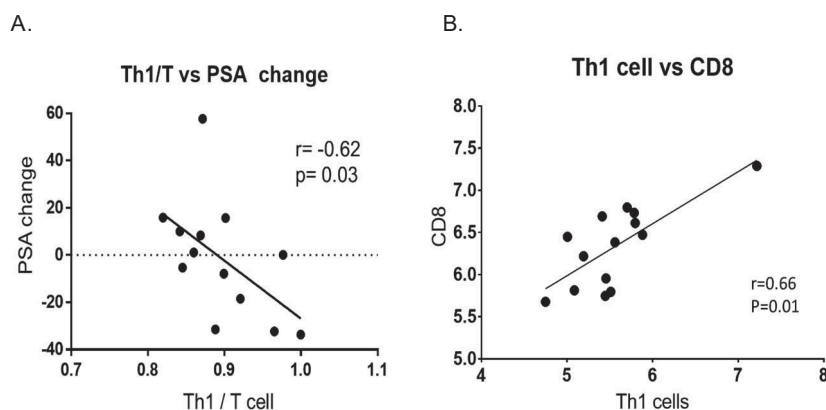


Figure 3. Association between serum PSA change on treatment and intratumoral Th1 score. (A) Correlation between serum PSA change and Th1/T immune gene score ratio in sipuleucel-T treated patients (n = 13) is shown. (B) Correlation between Th1 and CD8 immune cell scores in tumors from sipuleucel-T treated patients (n = 14).

PSA transcripts in patients with paired tissues obtained pre- and post-sipuleucel-T treatment. Because Th1 immune cell score was significantly correlated with CD8 T cell score ($P = 0.01$, **Figure 3B**), we hypothesize that both T cell subtypes are enriched in the tumor microenvironment of patients who had PSA response during neoadjuvant sipuleucel-T treatment.

Serum PSA increase is associated with transcriptional induction of inhibitory checkpoint genes after treatment

Even though immune cell score for Th1 cells were induced by sipuleucel-T, tumor infiltration by total T cells in post-treatment tissue was associated with PSA increase in serum ($p = 0.02$) (**Figure 4A**). We hypothesized that a proportion of the observed T cells were of a regulatory or exhausted phenotype, rather than of an activated phenotype. Indeed, there was also a trend of association between regulatory T cells and PSA increase in serum ($p = 0.10$) (**Figure 4B**). To this end, we performed differential expression gene analysis of the five paired pre- and post-sipuleucel-T treated tumor tissues, focusing on T cell function-related genes. The inhibitory

checkpoint genes CTLA4, TIGIT, and CEACAM6 were upregulated by sipuleucel-T treatment, while the T cell functional marker DPP4 was downregulated (**Figure 4C**). The level of gene expression of these inhibitory checkpoints in post-treatment RP tumors (N = 14) were significantly correlated with an increase in serum PSA after treatment (n = 14), ($p = 0.01$, <0.05 and 0.02 for CTLA4, TIGIT and CEACAM6, respectively, **Figure 4D**). These data suggest that the expression of these inhibitory checkpoint genes may hinder immune-mediated anti-tumor activity with sipuleucel-T treatment.

Discussion

We have previously shown that activated T cells are recruited into the prostate tumor microenvironment by sipuleucel.⁴ We now show that neoadjuvant sipuleucel-T elicits Th1 response that includes CXCL10 and a CD8 expression signature. To our knowledge, this is the first report to confirm that intratumoral Th1 immune response are specifically induced by sipuleucel-T treatment and are consistent with the Th1 immune responses that have been detected in the circulating

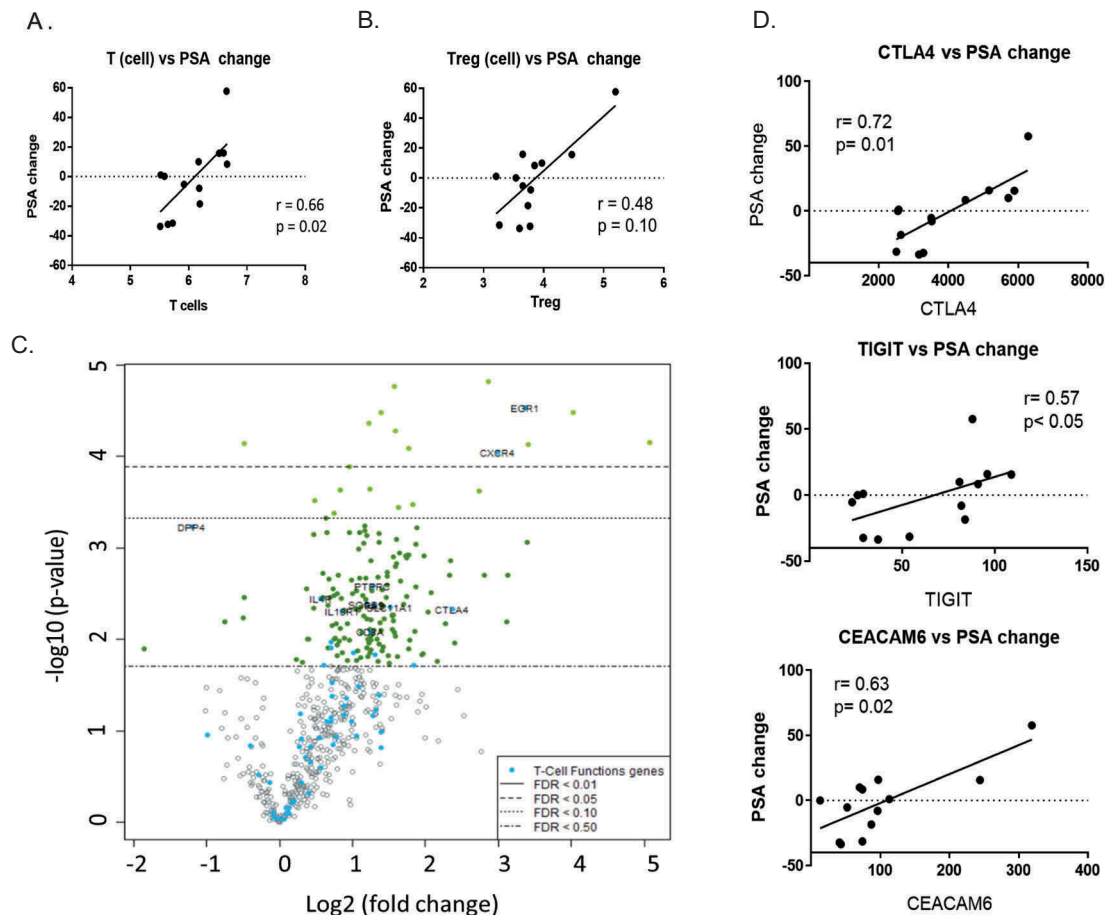


Figure 4. Association between serum PSA change during treatment and induction of inhibitory checkpoint genes in the tumor. (A) Correlation between intratumoral T cell immune gene score and serum PSA change is shown ($n = 13$). (B) Correlation between Treg cell immune gene score in the tumor and serum PSA change while on treatment is shown. (C) Differential expression of immune-related genes in post- vs. pre-sipuleucel-T prostate tumor tissues is shown ($n = 5$). T cell function-related genes are highlighted in blue. The X-axis indicates the log fold-change which estimates a gene's differential expression. (D) Correlation between serum PSA change and transcript levels of CTLA4, TIGIT and CEACAM6 in post-sipuleucel-T tumor are shown ($n = 13$).

T cells. Despite the induction of a Th1 signature, the induction of IFN-gamma was relatively modest, especially relative to the induction of CTLA4. This could reflect the kinetics of the response as surgical resection was performed 2–3 weeks following treatment. Alternatively, this blunted IFN-gamma response could reflect the immunosuppressive environment or induced immune checkpoints. Indeed, we have shown that lymphocytes induced by sipuleucel-T are localized are excluded from the tumor center.⁴ This phenotype can be associated with a TGF-beta signature in bladder cancer.⁸ While that presence of Th1 response associates with a PSA decrease on treatment, induction of inhibitory checkpoints was associated with PSA rise on treatment. We found a trend toward a positive correlation between TGFB1 and PSA change ($r = 0.465$, $p = 0.1150$). Interestingly, TGFB1 was positively correlated with CD8 cells ($r = 0.7143$, $p = 0.0054$). This could also reflect a mechanism of adaptive resistance.

Gene expression signatures associated with immune and/or clinical responses in other cancer types include different chemokines that contribute to T cell localizatio.^{9–11} Recently, Muthuswamy et al. reported that intratumoral CD8 T cells in untreated prostate tumors were positively correlated with CXCL9 and CXCL10 levels in the tumor microenvironmen.¹²

Consistent with this, we found that CXCL9 and CXCL10 are highly expressed in CD8-infiltrated prostate tumors following sipuleucel-T treatment. Furthermore, in situ hybridization showed CXCL10 mRNA expressing cells to be well colocalized with CD8 T cells. CXCL10 has been shown to be produced by M1 cells.⁷ Our data supported this report (Supplementary Figure 2); however, it remains to be further studied whether M1 cells actually secrete such functional chemokines. If this is the case, M1 cells could help convert prostate cancer from the prototypical cold tumor into a T cell inflamed tumor. Overall, these findings suggest sipuleucel-T treatment enhances CXCL9 and CXCL10 production, which in turn promote CD8 T cell recruitment into the tumor microenvironment.

In these exploratory analyses, we found that the induction of an intratumoral Th1 expression signature was inversely correlated with PSA progression suggesting that Th1 induction by sipuleucel-T could modulate PSA response. On the other hand, we also found that upregulation of the genes of inhibitory checkpoints CTLA-4, TIGIT and CEACAM6 were positively correlated with PSA progression, suggesting the possible role of these checkpoints in dampening treatment-induced immune responses. These could represent adaptive resistance mechanisms that could be targeted. The significance of PSA modulation observed in this study, which

were not large in magnitude, is unknown. Moreover, the overall number of patient samples examined was limited. Nevertheless, these results provide some rationale for clinical trials combining sipuleucel-T with immune checkpoint inhibition for prostate cancer, including the ongoing clinical trial combining sipuleucel-T with CTLA-4 blockade for metastatic castration resistant prostate cancer (NCT01804465). Continued correlative and mechanistic studies are needed to guide the design of clinical trials utilizing the most rationale combination strategies.

Materials and methods

Patients

Tissue samples were derived from a single-arm, multicenter phase II trial of neoadjuvant sipuleucel-T treatment in men with localized prostate cancer administered prior to planned R.⁴ Eligible patients had a normal complete blood count, adequate hepatic and renal function, tissue available from a pretreatment prostate biopsy, and were negative for HIV, HTLV-1 and -2, and hepatitis B and C. All subjects gave written informed consent to participate in the protocol approved by the Institutional Review Boards (IRBs) of each participating institution (NCT00715104). Subjects received sipuleucel-T at the standard two-week intervals for three planned doses prior to RP. Sipuleucel-T was started six to seven weeks prior to RP, allowing for a two- to three-week interval between the final infusion of sipuleucel-T and the RP.

Gene expression

RNA was extracted from FFPE tumor biopsy and RP sections using PureLink™ FFPE Total RNA Isolation Kit (Invitrogen) and was evaluated for gene expression using the nCounter® PanCancer Immune Profiling Panel (NanoString Technologies, Inc.), which interrogates 770 immune-related genes and associated controls. NanoString gene expression values were normalized using housekeeping genes included in the panel. The nSolver software (version 3.0) was used to perform all normalization, analyze gene expression, and calculate immune cell scores. Normalization was performed using the following house-keeping genes; PRPF38A, HPRT1, AGK, DDX50, HDAC3, TUBB, TLK2, AMMECR1L, CNOT10, TBP, MTMR14, ZKSCAN5, USP39, HX16, TMUB2, SF3A3, CNOT4, MRPS5, COG7, DNAJC14, ABCF1, ERCC3, EIF2B4, ZNF346, POLR2A, FCF1, PPIA, SDHA, ZC3H14, ALAS1, G6PD, TRIM39, NOL7, NUBP1, EDC3, SAP130, ZNF143, GUSB, CC2D1B, GPATCH3. Scores for each cell type were calculated based on the expression of the following genes; T cells: CD3G, CD96, SH2D1A, CD6, CD3D, LCK, CD2, and CD3E; CD8 cells: PRF1, D8A, GZMM, CD8B, and FLT3LG; Th cells: ATF2, NUP107; B cells: TNFRS 17, CD19, MS4A1, and BLK. Genes were tested for differential expression in response to each selected covariate. For each gene, a single linear regression was fit using all selected covariates to predict expression. Genes previously shown to be characteristic of various immune cell populations were used to measure these populations' abundance.⁶

Immunohistochemistry

Immunohistochemistry was performed using published methods.⁴ Stained slides were scanned with an automated microscope scanner (Aperio Scanscope XT, Aperio, Buffalo Grove, IL). For RP sections, tissue was designated into three distinct compartments: benign glands, tumor centers, and tumor interfaces. Five randomly selected fields (0.25 mm², original magnification 20×, 0.5 μm per pixel resolution) from each compartment were then captured from each slide with ImageScope software (Aperio). Tumor interfaces were defined as fields where malignant and benign glands were present. Automatic cell counts for single- and double-stained cells were determined for each field with color-specific algorithms in Axiovision software (Zeiss, Peabody, MA). The cell count for each compartment is reported as the mean for each of the five quantitated fields.

In situ hybridization

The RNAscope 2.5 duplex detection assays (Advanced Cell Diagnostics [ACD], Hayward, CA) were manually performed using target probes to CXCL10 and CD8a on post-sipuleucel-T RP sections according to the manufacturer's instruction. The RNA probes (Hs-CXCL10 and Hs-CD8A-C2) were designed by ACD to hybridize to CXCL10 and CD8a messenger RNA (mRNA) molecules. Probes Hs-POLR2A (encoding DNA-directed RNA polymerase II subunit RPB1) and Hs-PPIB (human peptidylprolyl isomerase B)-C2 from ACD were used as positive controls. DapB (bacterial dihydrodipicolinate reductase) from ACD was used as negative control. Briefly, FFPE tissue sections were deparaffinized and treated with Hydrogen Peroxide (10 min at room temperature (r.t.)), Target Retrieval (boiling for 15 min), and Protease Plus (30 min at 40°C) to allow for target probe access. Target probes were added onto the slides and incubated in the HybEZ oven (ACD) for 2 hours at 40°C to allow probe hybridization to RNA targets. The slides were washed and incubated with a series of signal amplification solutions; amplification (Amp) 1 (30 min at 40°C), Amp 2 (15 min at 40°C), Amp 3 (30 min at 40°C), Amp 4 (15 min at 40°C), Amp 5 (30 min at r.t.), and Amp 6 (15 min at r.t.). Signals to CD8a mRNA were generated by chromogenic reaction using Red-A/B (10 min at r.t.). The slides were washed and additionally amplified; Amp 7 (15 min at 40°C), Amp 8 (30 min at 40°C), Amp 9 (30 min at r.t.), and Amp 10 (15 min at r.t.). Signals to CXCL10 mRNA were generated using Green-A/B (10 min at r.t.). The slides were counterstained with hematoxylin and mounted with VectaMount. The stained slides were examined by bright field microscopy.

Statistical analysis

Two-tailed paired t-test was used to assess overall differences in mean IHC results or Nanostring scores between two groups. The Spearman rank order correlation was used to evaluate the relationships between Nanostring scores and IHC results. All statistical tests were two-sided and $p < 0.05$ was considered statistically significant. There was no adjustment for multiple testing issue unless noted in Nanostring gene expression data analysis. Statistical analysis was performed using GraphPad

Prism version 7.00 for Windows, GraphPad Software, La Jolla California USA, www.graphpad.com.

Acknowledgments

This work has been supported by National Cancer Institute (NCI) grants R01CA163012, R01CA194511, and a Prostate Cancer Foundation Challenge Grant.

Funding

This work was supported by the Prostate Cancer Foundation (PCF) [Movember Challenge Grant]; HHS | NIH | National Cancer Institute (NCI) [R01CA223484]; HHS | NIH | National Cancer Institute (NCI) [R01CA163012].

ORCID

Katsunobu Hagihara  <http://orcid.org/0000-0003-0094-2543>
Lawrence Fong  <http://orcid.org/0000-0002-6428-428X>

References

1. GuhaThakurta D, Sheikh NA, Fan LQ, Kandadi H, Meagher TC, Hall SJ, Kantoff PW, Higano CS, Small EJ, Gardner TA et al. Humoral immune response against nontargeted tumor antigens after treatment with sipuleucel-T and its association with improved clinical outcome. *Clin Cancer Res.* 2015;21(16):3619–3630. doi:10.1158/1078-0432.CCR-14-2334.
2. Higano CS, Schellhammer PF, Small EJ, Burch PA, Nemunaitis J, Yuh L, Provost N, Frohlich MW. Integrated data from 2 randomized, double-blind, placebo-controlled, phase 3 trials of active cellular immunotherapy with sipuleucel-T in advanced prostate cancer. *Cancer.* 2009;11516: 3670–3679. doi:10.1002/cncr.24429
3. Kantoff PW, Higano CS, Shore ND, Berger ER, Small EJ, Penson DF, Redfern CH, Ferrari AC, Dreicer R, Sims RB et al. Sipuleucel-T immunotherapy for castration-resistant prostate cancer. *N Engl J Med.* 2010;363(5):411–422. doi:10.1056/NEJMoa1001294.
4. Fong L, Carroll P, Weinberg V, Chan S, Lewis J, Corman J, Amling CL, Stephenson RA, Simko J, Sheikh NA. et al. Activated lymphocyte recruitment into the tumor microenvironment following preoperative sipuleucel-T for localized prostate cancer. *J Natl Cancer Inst.* 2014;10611: doi:10.1093/jnci/dju268
5. Sheikh N, Cham J, Zhang L, DeVries T, Letarte S, Pufnock J, Hamm D, Trager J, Fong L. Clonotypic diversification of intratumoral T cells following sipuleucel-T treatment in prostate cancer subjects. *Cancer Res.* 2016;7613: 3711–3718. doi:10.1158/0008-5472.CAN-15-3173
6. Danaher P, Warren S, Dennis L, D'Amico L, White A, Disis ML, Geller MA, Odunsi K, Beechem J, Fling SP. Gene expression markers of tumor infiltrating leukocytes. *J Immunother Cancer.* 2017;518. doi:10.1186/s40425-017-0215-8
7. Burkholder B, Huang RY, Burgess R, Luo S, Jones VS, Zhang W, Lv ZQ, Gao CY, Wang BL, Zhang YM, et al. Tumor-induced perturbations of cytokines and immune cell networks. *Biochim Biophys Acta.* 2014;1845(2):182–201. doi:10.1016/j.bbcan.2014.01.004.
8. Mariathasan S, Turley S, Nickles D, Kadel EE, Koeppen H, Yuen K, Castiglioni A, Astarita J, Cubas R, Jhunjhunwala S, et al. A balance of genomic instability, tumour-immune topography and TGF- β signaling governs response to PD-L1 blockade in metastatic bladder cancer. *Nature.* 2018. doi:10.1038/nature25501
9. Harlin H, Meng Y, Peterson AC, Zha Y, Tretiakova M, Slingluff C, McKee M, Gajewski TF. Chemokine expression in melanoma metastases associated with CD8+ T-cell recruitment. *Cancer Res.* 2009;697: 3077–3085. doi:10.1158/0008-5472.CAN-08-2281
10. Messina JL, Fenstermacher DA, Eschrich S, Qu X, Berglund AE, Lloyd MC, Schell MJ, Sondak VK, Weber JS, Mule JJ. 12-Chemokine gene signature identifies lymph node-like structures in melanoma: potential for patient selection for immunotherapy? *Sci Rep.* 2012;2765. doi:10.1038/srep00765
11. Ulloa-Montoya F, Louahed J, Dizier B, Gruselle O, Spiessens B, Lehmann FF, Suci S, Kruit WH, Eggermont AM, Vansteenkiste J, et al. Predictive gene signature in MAGE-A3 antigen-specific cancer immunotherapy. *J Clin Oncol.* 2013;31(19):2388–2395. doi:10.1200/JCO.2012.44.3762.
12. Muthuswamy R, Corman JM, Dahl K, Chatta GS, Kalinski P. Functional reprogramming of human prostate cancer to promote local attraction of effector CD8(+) T cells. *Prostate.* 2016;7612: 1095–1105. doi:10.1002/pros.23194